Published in final edited form as:
Biomaterials. 2011 July ; 32(21): 4903–4913. doi:10.1016/j.biomaterials.2011.03.027.

Engineering Chemoattractant Gradients Using Chemokine-Releasing Polysaccharide Microspheres

Yana Wang[1] and **Darrell J. Irvine**[2,3,4,5,6]

[1] Department of Chemical Engineering, Massachusetts Institute of Technology, Cambridge, MA, USA

[2] Department of Biological Engineering, Massachusetts Institute of Technology, Cambridge, MA, USA

[3] Department of Material Science and Engineering, Massachusetts Institute of Technology, Cambridge, MA, USA

[4] Koch Institute for Integrative Cancer Research, Massachusetts Institute of Technology, Cambridge, MA, USA

[5] Ragon Institute of Massachusetts General Hospital, MIT and Harvard University, Boston, Massachusetts, USA

[6] Howard Hughes Medical Institute, Chevy Chase, Maryland, USA

Abstract

Spatial and temporal concentration gradients of chemoattractants direct many biological processes, especially the guidance of immune cells to tissue sites during homeostasis and responses to infection. Such gradients are ultimately generated by secretion of attractant proteins from single cells or collections of cells. Here we describe cell-sized chemoattractant-releasing polysaccharide microspheres, capable of mimicking chemokine secretion by host cells and generating sustained bioactive chemokine gradients in their local microenvironment. Exploiting the common characteristic of net cationic charge and reversible glycosaminoglycan binding exhibited by many chemokines, we synthesized alginate hydrogel microspheres that could be loaded with several different chemokines (including CCL21, CCL19, CXCL12, and CXCL10) by electrostatic adsorption. These polysaccharide microspheres subsequently released the attractants over periods ranging from a few hrs to at least 1 day when placed in serum-containing medium or collagen gels. The generated gradients were able to attract cells more than hundreds of microns away to make contact with individual microspheres. This versatile system for chemoattractant delivery could find applications in immunotherapy, vaccines and fundamental chemotaxis studies *in vivo* and *in vitro*.

1. Introduction

Directed lymphocyte trafficking is a key part of development, homeostasis and ongoing immune responses within primary lymphoid organs, secondary lymphoid organs, and

Correspondence should be addressed to D.J.I. (djirvine@mit.edu).

peripheral tissues. The migration of lymphocytes is controlled in part by a family of host chemotactic molecular signals, chemokines [1–4]. Chemokines are secreted by host cells and diffuse into the surrounding tissue to establish soluble and/or immobilized concentration gradients [5]. These attractants are also displayed on the surfaces of endothelial cells at sites of inflammation and on blood vessels in lymphoid organs, providing a key signal for arrest of leukocytes on the endothelial wall for entry into tissues from the blood [5, 6]. Lymphocytes expressing cognate chemokine receptors sense concentration differences within tissues and migrate up the gradient toward areas of high chemokine concentration [7], a process called chemotaxis. Chemokines can also trigger chemokinesis, non-directed migration stimulated by chemokines present at stimulatory levels without the presence of functional spatial gradients [8, 9].

Through an understanding of fundamental principles of leukocyte trafficking, a variety of therapeutic applications are being developed, such as vaccine adjuvants, anti-tumor reagents, and anti-inflammatory treatments [10]. In vaccination and cancer therapy, a promising approach is to locally engineer chemokine gradients with the goal of drawing immune cells to tumors or immunization sites. For example, DNA or vaccinia virus vaccines co-injected with DNA plasmids encoding the chemokines CCL21 or CCL19 increased the protective immune response against Herps Simplex Type 1 Virus [11]. Intratumoral injection of leukocyte-attracting recombinant chemokines, such as CCL21 [12] or CCL16 [13], have shown promising anti-tumor effects. Intratumoral injection of dendritic cells transfected to express CCL21 [14] or including CCL21 retroviral particles in adoptive T-cell therapy [15] have shown improved effects in tumor rejection. The adenoviral delivery of CCL16 synergized with the use of CpG and anti-IL-10 antibody [16] to promote the accumulation of dendritic cells and macrophages at tumor sites and elicited cascading innate and adaptive immune responses to reject large tumors. Biomaterials may have a key role to play in this setting, by providing the means to gain greater control over engineered chemoattractant gradients relative to transfected cells or bolus attractant injection. Kumamoto et al. showed that implanted poly(ethylene-co-vinyl acetate) rods releasing the mature dendritic cell chemoattractant CCL19 and a tumor antigen could elicit promising anti-tumor immunity [17]. The immature dendritic cell chemoattractant CCL20 has also been encapsulated in biodegradable *in situ*-crosslinking hydrogels comprised of Dextran vinyl sulfone and reactive polyethylene glycol [18] to attract antigen presenting cells to an injection site during vaccination. Controlled release materials also offer the potential to engineer gradients for basic studies of chemotaxis *in vitro*, such as demonstrated by Kress et al. who used optical tweezer manipulation of attractant-releasing PLGA microspheres as a strategy to finely position attractant gradients relative to responding cells [19].

We previously reported the use of poly (lactide-co-glycolide) (PLGA) microspheres loaded with the chemokine CCL20 or bacterial formyl peptides to generate local dendritic cell chemoattractant gradients [20]. This system was attractive as it employed a well-established fully bioresorbable material for chemokine release, but the loading of chemokines (typical of many protein cargos in PLGA particles) was limited to on the order of ~1 wt% of the microspheres, and we found that obtaining functional release of many other candidate chemokines of interest was problematic, likely due to the harsh microenvironment within eroding PLGA particles [21–23]. Thus, we searched for an alternative system that could more efficiently entrap chemokines with higher net bioactivity, and provide “point-source” release of a broader range of attractants to engineer chemokine gradients *in vitro* and *in vivo*.

Apropos of this challenge, we recently developed injectable formulations of the well-known anionic polysaccharide biomaterial alginate, based on mixing alginate aqueous solutions with suspensions of calcium alginate microspheres; the microspheres served as local sources of excess calcium that crosslinked the surrounding solution over a period of minutes via ion

exchange [24, 25]. The favorable *in vivo* properties of these alginate materials and the structural similarities of alginate to native glycosaminoglycans (GAGs) led us to hypothesize that alginate microspheres could be utilized not only as ion reservoirs, but also as carriers for reversible loading and controlled release of chemokines. Chemokines are generally cationic small proteins (~8–20 KDa), which bind to GAGs in the extracellular matrix (ECM) or on the surface of cells. Many chemokines bind the sulfated and carboxylic acid residues of heparan sulfate (HS) and its analogs, in some cases with nM affinity, and proteoglycan binding has been formally shown to be essential for the *in vivo* activity of some chemokines [26–28]. We reasoned that similar interactions between chemoattractants and acid groups of alginate microspheres would enable loading/release of chemokines, and the ubiquitous nature of charge-mediated chemokine binding to matrix would allow this approach to be applied to many host attractants. Providing support for this concept, alginate has been used to encapsulate many therapeutic proteins via ionic interactions, such as basic fibroblast growth factor (bFGF) [29], transforming growth factor-β_1 (TGF-β_1) [30], nerve growth factor (NGF) [31], and platelet-derived growth factor (PDGF) [32].

Here, we report on studies testing this hypothesis and demonstrating a simple approach to create chemokine-loaded microspheres that potently chemoattract immune cells. We evaluated loading/release of several chemokines important in immunity, including CCL19, CCL21, CXCL12 and CXCL10. We employed simulations of the gradient field generated around individual microspheres coupled with Boyden chamber assays and direct videomicroscopy imaging of human leukocytes migrating near alginate microspheres to test the functionality of these attractant particles, and defined conditions for long-lived and long-ranged attraction of human T-cells or dendritic cells to isolated microspheres or collections of particles.

2. Materials and methods

2.1. Materials

LF120M alginates (70–150 mPa·s with 45–55% guluronic acid units) were obtained from FMC Biopolymers (Sandvika, Norway). 2,2,4-Trimethylpentane (*iso*-octane, ChromAR, 99.5%) was obtained from Mallinckrodt Baker (Phillipsburg, NJ). Calcium chloride dehydrate, Sorbitane monooleate (Span 80), Tween 80, HEPES buffer, and lipopolysaccharide (LPS) from *Escherichia coli*, lectin from *Phaseolus Vulgaris* (PHA) were purchased from Sigma–Aldrich (St. Louis, MO). Bovine type I collagen (*PureCol*® stock solutions ~3 mg/ml) was obtained from Advanced Biomatrix (Tucson, Arizona). Human recombinant CCL21, CCL19, CXCL12, GM-CSF and detection ELISA Duoset® kits were purchased from R&D systems (Minneapolis, MN). Mouse CXCL10 and human IL-4 recombinant proteins were obtained from Peprotech (Rocky Hill, NJ) and mouse CXCL10 detection ELISA kits were purchased from R&D systems. Human recombinant IL-2 was obtained from Chiron (Emeryville, CA). RPMI-glutamax, Alexa fluor 488 and Alexa fluor 555 small scale labeling kits were purchased from Invitrogen (Carlsbad, CA). Polydimethylsiloxane (PDMS) rubber culture chambers were cast from Sylgard 184 silicone elastomer kits (Dow Corning, Midland, MI). Low autofluorescence phenol red-free RPMI powder was obtained from Mediatech (Manassas, VA). Ficoll-paque for lymphocyte isolation was purchased from GE Healthcare (Uppsala, Sweden). All materials were used as received unless otherwise noted.

2.2. Synthesis of alginate microspheres

Alginate microspheres were synthesized using a procedure we previously reported [24, 25]: Briefly, alginate was dissolved in phosphate buffered saline (PBS) pH 7.4 (1% wt/vol) and passed through a sterile 0.45 μm syringe filter. The solution (400 μl) was added dropwise

and homogenized at 25°C for 3 min at 8000 rpm (UltraTurrax T25 homogenizer, IKA Works) in 35 ml of iso-octane containing 1.5 ml Span 80 and 0.5 ml Tween 80, and then 25 μl $CaCl_2$ (5% wt/vol) solution was added dropwise followed by 4 min homogenization. The resulting calcium alginate microspheres were collected by centrifugation and washing 2X with 35 ml *iso*-octane followed by washing 3X with 1 ml deionized water, then stored at a stock concentration of 5×10^6 microspheres/ml in deionized water at 4°C until use.

2.3. Characterization of microspheres

The size distributions of alginate microspheres in deionized water were determined using a Horiba laser scanning particle size distribution analyzer LA-950V2. The morphology of alginate microspheres was characterized using a Zeiss Axiovert 200 epi fluorescence microscope, and the number concentration of alginate microspheres was quantitated via a haemocytometer.

2.4. Loading of chemokines in alginate microspheres

To determine the net surface charge of candidate chemokines, crystal structures of chemokines available from the Protein Data Bank were inspected (www.pdb.org, structures: CXCL12: 2KED; CXCL10:1LV9) using Star Biochem software (MIT, Cambridge, MA) to identify surface-exposed residues. For CCL21 and CCL19 whose crystal structures are not yet available, it was assumed that all charged residues were exposed on the surface, consistent with many other chemokines [33]. The isoelectric point of the chemoattractants was calculated based on the published amino acid sequence.

Before use, chemokine was loaded into the alginate microspheres by adsorption: alginate particle suspensions were spun down, the supernatant discarded, and the particles were resuspended in a concentrated chemokine solution at 5×10^6 particles/ml (equivalent to 0.04 mg/ml alginate) for 90 min (except where otherwise noted) on a rotator at 4°C. Chemokine stock solutions were diluted in PBS with 0.1 wt% BSA for these loading incubations. After the incubation period, the microspheres were washed 3X with 1 ml phenol red-free RPMI 1640 medium containing 10% fetal calf serum (FCS) to remove unbound chemokine. The chemokine-loaded particles were then resuspended in phenol red-free RPMI at 5×10^6 particles/ml and used for release or imaging studies. The amount of chemokine loaded was evaluated by subtracting the quantity of chemokine detected in the washing supernatant (analyzed by ELISA) from the total amount of attractant initially added in the loading process. We confirmed that this analysis gave similar results to measurements obtained by digesting microspheres with alginate lyase (10 ng/ml alginate lyase for 20 min at 37 °C) and measuring the loaded chemokine directly.

2.5. Release of chemokines from alginate microspheres

Kinetics of chemokine release from the microspheres were determined by suspending 5×10^4 chemokine-loaded alginate microsphere in 1 ml releasing buffer (as noted in the text) and incubating at 37 °C on an orbital shaker (200 rpm). At each time-point, the particles were pelleted, the supernatant collected for analysis, and fresh buffer was added to approximate sink conditions during release. The amount of chemokine in supernatant samples was measured by ELISA.

In order to simulate the gradient fields developing around individual microspheres in our chemotaxis assays, we calculated the apparent diffusion constant for chemokine within individual alginate microspheres. This effective diffusivity, D_{eff}, was determined by fitting the measured fraction of chemokine released at each time-point using a short term solution for Fick's Second Law applied to spherical geometry in sink conditions (valid for time-points when < 40% of the total release has occurred) [34]:

$$\frac{M_t}{M_\infty} = \sum_i w_i \left(6 \left(\frac{D_{eff} t}{\pi R_i^2} \right)^{\frac{1}{2}} - \frac{3 D_{eff} t}{R_i^2} \right)$$

where M_t is the amount of chemokine release at time t, M_∞ is the total amount released at infinite time (i.e. total amount loaded in the particles), and w_i is the weight fraction of microspheres with radius R_i, summed over the distribution of all microsphere sizes. This analysis accounted for the polydispersity of the microspheres and the sum over all particle sizes was carried out using the experimentally determined size distribution of the particles. Data was fit using the built-in nonlinear regression algorithm of Prism 5.0 software (GraphPad Software).

2.6. Cells

Peripheral blood mononuclear cells (PBMCs) were isolated by ficoll gradient centrifugation of whole blood or unpurified buffycoats from healthy anonymous donors (Research Blood Components, Boston, MA). Resting T-cells were isolated by magnetic sorting (pan human T-cell negative selection kit, Miltenyi, Auburn, CA) and cultured in RPMI-glutamax (Invitrogen, Carlsbad, CA) containing 10 mM HEPES and 10% FCS for 18 hr prior to use. Activated T-cells were prepared by culturing PBMCs at 7×10^6 cells in 3 ml RPMI medium with 10% FCS and stimulated with 1 μg/ml PHA for two days. On day 3, activated PBMCS were ficolled to remove dead cells, followed by magnetic sorting using T-cell isolation kit from Miltenyi. The purified human T-cells were cultured at 1×10^6/ml in 10% FCS containing RPMI medium with 100 U/ml IL-2 and used on day 4. To prepare monocyte-derived human dendritic cells (DCs), monocytes were isolated from PBMCs by magnetic selection (CD14 microbead positive selection kit, Miltenyi) and then cultured at 1×10^6 cells/ml in RPMI medium containing 25 ng/ml recombinant human IL-4 and 100 ng/ml recombinant human GM-CSF for 7 days to generate monocyte-derived DCs. Medium was changed every other day; on day 5, 100 ng/ml LPS was added to mature the DCs, and the cells were used for experiments on day 7. Activated human T-cells or dendritic cells used for imaging were labeled with 3.3 μM CMTPX (Invitrogen) prior to experiments according to the manufacturer's instructions.

2.7. Preparation of collagen hydrogels

Soluble collagen (3.0 mg/ml stock acid solution) was mixed with 0.1 M sterile NaOH and 10X phenol red-free RPMI in a 8:1:1 vol ratio to achieve pH 7.2, then this mixture was combined with FCS (final conc. 10% vol/vol) and phenol red-free RPMI at a ratio of 3:0.33:0.67 to obtain a final collagen concentration of 1.8 mg/ml. This collagen precursor solution was mixed with cells and/or alginate microspheres at desired concentrations and incubated at 37°C to allow polymerization of the solution into a fibrillar collagen gel containing the desired concentration of suspended cells and alginate particles.

2.8. Modified Boyden chamber chemotaxis assay

T-cells (5×10^4 cells in 50 μl) in RPMI medium with 10% FCS or 1.8 mg/ml collagen solution were applied to the top compartment of 96-well polycarbonate filter plates with 5 μm pore sizes (Neuro Probe, Gaithersburg, MD); recombinant chemokines or chemokine-loaded alginate microspheres in RPMI with 10% FCS (30 μl) were added to the lower compartments of each chamber. CCL21-loaded alginate microspheres (2.5 μg/mg alginate) were 10X serial diluted from 5×10^6 particles/ml (total CCL21 loaded on alginate microsphere was equivalent to 10 μg/ml soluble CCL21) to generate dose titrations. After a 2 or 4 hr incubation at 37°C for cells added in medium or collagen, respectively, cells

remaining on top of the filters were removed by gentle washing and those that migrated to the bottom chamber were quantified using a Cyquant cell enumeration kit (Invitrogen) following the manufacturer's instructions.

2.9. Microsphere depot videomicroscopy chemotaxis assay

Custom culture wells composed of two interconnected cylindrical wells each ~4.5 mm in diameter and ~3 mm in depth were prepared by sealing PDMS rubber molds against #1 borosilicate glass coverslip labtek chamber slides (Nalge Nunc Labtek). Collagen precursor solution (30 μl) mixed with 5×10^4 alginate particles loaded with 0.8 μg CCL21 (50% was Alexa fluor 488-labeled) was deposited in one chamber of the PDMS mold and incubated at 37°C for 5 min, then 30 μl of collagen mixed with CMTPX-labeled LPS-matured dendritic cells at 1×10^6 cells/ml was deposited in the adjoining chamber. The labtek slide was immediately placed in a 5% CO_2, 37°C humidified environmental chamber on a Zeiss Axiovert 200 inverted fluorescence microscope. Samples were imaged in time-lapse, employing a computer-controlled robotic stage to collect images of 9 adjacent 334 × 448 μm fields of view at 20X across the interface between the chemokine-loaded well and cell-loaded well in rapid succession. Brightfield, green and red fluorescence images were collected from all 9 fields every 5 min for 10 hrs.

2.10. Isolated microspheres videomicroscopy chemotaxis Assay

Single custom culture wells containing one cylindrical well (~ 4.5 mm in diameter and ~3 mm in depth) were sealed to glass coverslip imaging chambers similarly as described in 2.9. Collagen precursor solution (30 μl) mixed with activated CMTPX-labeled human T-cells (final conc., 3×10^6 cells/ml) and chemokine-alginate microspheres (final conc., 1×10^4 particles/ml) was deposited into the pre-heated culture well and then imaged in time-lapse. One 334 × 448 μm field containing a single alginate microsphere was selected for imaging in time-lapse in each sample. Brightfield and red fluorescence images were taken every minute for 3 to 6 hrs.

2.11. Isolated microsphere chemokine gradient modeling

The release of chemokines and development of concentration gradient fields around individual alginate microspheres embedded in collagen hydrogels was simulated by solving Fick's second law of diffusion for a single attractant-releasing microsphere centered in a cubic space of dimension *a* using the *transport of diluted species* module in COMSOL modeling software (COMSOL Inc., Burlington, MA). The dimension of the space, *a*, was taken as the mean distance between microspheres dispersed within a collagen matrix at a total number concentration C_{MS}:

$$a=c_{MS}^{-1/3}$$

The COMSOL model solved differential equations for diffusion of chemokine with an initial uniform concentration of attractant in the beads (C_o) at time zero and no flux at the boundaries:

$$\frac{dc}{dt}=D\nabla^2C$$
$$t\le 0, C=C_0, r\le R \text{ and } C=0, r>R$$
$$t>0, \text{ no flux at boundary}; D=D_{eff}, r\le R \text{ and } D=D_c, r>R$$

where D_c is the diffusivity of chemokine in collagen and D_{eff} is the effective diffusivity of chemokine within the alginate microsphere, defined from our experimental measurements as

described in section 2.5 above. Following prior work [20], because the porosity of the fibrillar collagen matrix is on length scales much greater than the size of the chemokine and we found no evidence for interactions of the chemokines studied with the type I collagen used here in ELISA binding assays (data not shown), D_c was taken as half the diffusivity of chemokine in water, D_o. D_o was estimated using the empirical relationship [35, 36]:

$$D_0=\frac{A}{MW^{1/3}}$$

where A is a constant, 2.82×10^{-5} cm^2/s (g/mol)$^{1/3}$, and MW is the protein molecular weight. These relationships gave $D_c^{CCL21} = 6.5\times10^{-7}$ cm^2/s and $D_c^{CXCL12} = 7.45\times10^{-7}$ cm^2/s. Solutions of the diffusion equations were solved for free triangular FEM mesh points of maximum spacing, 8 μm and minimum spacing, 16 nm.

As suggested in previous studies [35, 37], the chemokine receptor occupancy (*B*), defined as the concentration of receptor with bound chemokine (*RC*) divided by the concentration of total receptor on the cell surface (R_{max}) was calculated by assuming chemokine-receptor binding reaches equilibrium:

$$B=\frac{RC}{R_{\max}}=\frac{C}{K_d+C}$$

where K_d is the binding affinity of chemokine and receptor. CCL21 binding affinity for CCR7 has been measured on CCR7-transfected cells or on human T-cells, with estimates ranging from 1 nM to 10 nM [38–40] and here we chose to use K_d = 5 nM. The affinity between CXCR4 and CXCL12 were reported to be 1.8 nM or 4 nM in [41, 42], and 3 nM was used here. The receptor occupancy gradient was derived as:

$$\frac{dB}{dr}=\frac{K_d}{(K_d+C)^2}\cdot\frac{dC}{dr}$$

2.12 Single-cell migration analysis

To analyze cell migration in the two-well conjoined gel chemotaxis imaging assay and isolated microsphere chemotaxis imaging assay, individual dendritic cells or T-cells were tracked for the time window indicated in the text using Image J (NIH, Bethesda, MD). The chemotactic index (CI) was defined as the displacement of each cell in the direction of the attractant gradient divided by the total path length it traveled over the observation time [43]. In the conjoined gel chemotaxis assay, an instantaneous chemotactic index (ICI) was determined for the 20 cells analyzed in the field of view 1 mm away from the interface between the cell source and attractant source gels. The ICI was defined as the distance traveled by the T-cell toward the attractant source gel in one increment of observation time (5 min) divided by the total displacement of the cell in that interval. These single ICI values were averaged over all time steps to obtain a mean CI for the total 20 cells tracked in each condition.

In the isolated microsphere chemotaxis assay, ICI values were determined for each cell analyzed at each time point over a 1 hr time of observation, and these values were recorded along with the starting position of each cell at that time step. To capture the effect of differences in the chemoattractant gradient as a function of distance from the bead, the ICIs were then binned in 25 μm intervals of distance of the cell from the bead and ICI values within each bin were averaged to capture the mean strength of chemotaxis as a function of

position in the gradient over the 1 hr analysis time: i.e. we averaged all ICI values collected for cells 0–25 μm from bead, 25–50 μm away, 50–75 μm away, etc. For cells whose starting position were beyond 200 μm were binned together and labeled 250 μm.

2.13 Statistical analysis

Measured values are expressed as means ± standard errors (SE). Levels of significance for comparing average CI and velocity of dendritic cells in conjoined gel assay were calculated using an unpaired two-tailed *t* test. Level of significance for comparing mean values of ICI of T-cell migration in isolated microsphere assay to hypothetical value zero were calculated using one sample *t* test. Level of significance for comparing mean values of ICI as a function of distance to microspheres was calculated using paired *t* tests. All calculations were made using GraphPad Prism 5.0.

3. Results

3.1. Chemokine alginate microsphere formulation

To obtain cell-sized alginate particles, we employed a water-in-oil emulsion synthesis approach we described previously [25, 44] to prepare calcium alginate microspheres: As depicted in Supplementary Fig. 1, an aqueous alginate solution was emulsified in *iso*-octane with lyophilic surfactants, and the alginate emulsion droplets were ionically crosslinked by the subsequent addition of aqueous calcium chloride. The resulting alginate particles had a spherical morphology (as seen by brightfield microscopy, not shown) and diameters of 31±12 um in the hydrated state (Fig. 1A), as measured by laser diffraction.

Chemokines are typically small basic proteins and many are known to bind with substantial affinity to anionic extracellular GAGs [26, 45–47]. We reasoned that the anionic polysaccharide chains within alginate microspheres could serve as surrogates for native mammalian proteoglycans and provide multivalent binding sites to support reversible loading of chemokines by adsorption into pre-synthesized alginate particles. We chose human CCL21 (12 kDa, net charge +16) as a model chemokine to study the loading and release of attractants from alginate microspheres, due to its relevance in immune cell trafficking to lymphatics and lymphoid tissues [48–52] and its known high affinity for GAGs [53, 54]. As shown in Fig. 1B for the particular case of alginate microspheres incubated with a 20 μg/ml CCL21 solution, particles rehydrated with concentrated CCL21 solutions rapidly equilibrated with the chemokine, and maximal levels of attractant were bound within 30 min. This rapid binding equilibration is consistent with prior studies where ionic adsorption has been utilized to load charged proteins in alginate matrices [55]. Using 90 min incubations of particles with chemokine, as the quantity of protein mixed with particles was decreased from 50 μg CCL21/mg alginate to less than 10 μg chemokine/mg polysaccharide, the loading efficiency of CCL21 increased from 55% to greater than 95% (Fig. 1C). Flow cytometry analysis of alginate microspheres loaded with fluorescently-labeled CCL21 showed uniform shifts of the entire particle distribution to brighter fluorescence as increasing quantities of CCL21 were added to a fixed concentration of particles, indicating that the entire population of microspheres contributed uniformly to chemokine binding (Fig. 1D). The average attractant loading in individual alginate microspheres was 16 pg CCL21 per particle (average particle size of 31 μm) for the case of adding 25 μg CCL21 per mg alginate particles. Scatchard plots of the ratio of bound to equilibrium free CCL21 vs. bound CCL21 (Fig. 1E) were concave, suggesting negative cooperativity in the adsorption process. Consistent with this finding, the adsorption data was fit well by an empirical Freundlich isotherm model (solid line through the data in Fig. 1E) [56], which captures the binding of an adsorbent to multiple sites in a matrix with heterogeneous binding energy:

$$y=\alpha C^{1/n}$$

where C is the free chemokine concentration in the loading solution, y is the concentration loaded in alginate microspheres, α is the adsorption coefficient (quantifying the adsorption capacity) and $1/n$ denotes the adsorption exponent indicating the adsorption intensity. Using nonlinear regression we obtained α as 1.349 ± 0.2443 ml/mg alginate, $1/n$ as 0.8577 ± 0.05307 (quality of fit R square = 0.9972). Similar heterogeneous binding site equilibria and negative cooperativity in binding have been measured for other protein-ionic matrix adsorption studies [57].

3.2. Kinetics and bioactivity of CCL21 release from alginate microspheres

The kinetics of CCL21 release from alginate microspheres was characterized by bulk measurements of chemokine in the supernatant of particle suspensions over time. We first assessed the impact of medium ionic strength on chemokine release. Consistent with electrostatic-mediated binding of CCL21 to the alginate matrix, increasing the ionic strength of the release buffer increased the rate of attractant release from the particles (Fig. 2A). Next, we evaluated the effect of the amount of chemokine loaded on the release rate (Fig. 2B); the net amount of CCL21 released at any time was proportional to the quantity loaded. We fit the release data over 5 hrs to a model applying Fick's law to a polydisperse collection of microspheres with the experimentally-determined size distribution to obtain an effective diffusion constant for chemokine in the alginate matrix [57]. This model fit the data well (Fig. 2D) with $D_{eff} = (4.73 \pm 0.26) \times 10^{-13}$ cm^2/s for particles incubated with 25 μg CCL21/mg alginate during loading. This experimentally-derived D_{eff} provided the means for modeling the chemokine gradient formed around individual particles (discussed in detail below).

We next used a modified Boyden chamber chemotaxis assay [35] to evaluate the bioactivity of chemokine released from alginate microspheres for attracting resting human T-cells. T-cells suspended in medium or fibrillar collagen gels were placed on the top surface of 5 μm-pore membranes, and migration through the filters in response to soluble CCL21 or equivalent total doses of CCL21 loaded in alginate microspheres in the lower wells was quantified after 2 hr (for cells in medium) or 4 hr (for cells in collagen). The objective of these measurements was only to obtain a baseline assessment of whether attractant released from the microspheres was functional for chemoattraction, since the concentration gradients produced in this assay by soluble CCL21 are expected to be very different from that generated by the CCL21-releasing microspheres [20]. As expected [38–40], soluble CCL21 elicited chemotaxis of T-cells when added to the lower well of the migration chambers at doses of 10 ng/ml, with attraction plateauing at 100 ng/ml or higher concentrations for cells in medium (Fig. 3A). When cells were added to filters in collagen (requiring migration through the collagen matrix to cross the filters), lower levels of net migration were detected but a similar trend of increasing migration with increasing CCL21 dose were observed, with a plateau in response at 1 μg/ml attractant. Importantly, CCL21-releasing alginate particles also triggered dose-dependent chemoattraction of T-cells in both medium and collagen gels, demonstrating activity of the released protein (Fig. 3A). Note that equivalent migration is not expected here both because of the different gradients generated by soluble attractant vs. microspheres and also because only 10–15% of the CCL21 is released from the microspheres over these time courses.

Sustained cell migration through 3D extracellular matrix is more relevant for gauging the potential utility of alginate microspheres for engineering chemotaxis *in vivo* than migration very short distances through filter membranes [58]. Thus, as a second bioactivity assay we

also measured single-cell migration paths for human dendritic cells (DCs) suspended in collagen gels and exposed at time zero to an adjacent (physically associated) gel containing either soluble chemokine or CCL21-loaded alginate microspheres (schematically illustrated in Fig. 3B). Maturing DCs in the periphery express CCR7 and migrate to lymph nodes in response to CCL21 produced by lymphatic vessels in the local tissue [6, 59]; we used DCs stimulated with LPS to trigger CCR7 expression (Supplementary Fig. 2A) for this assay. 5×10^4 alginate microspheres loaded with a total of 0.8 μg CCL21 (releasing ~0.16 μg over 10 hr) were introduced in the "attractant source" side gel at time zero, and migration of DCs in the adjacent "cell source" gel and crossing into the adjoining gel were tracked for 10 hr by videomicroscopy. DCs exposed to microsphere-generated gradients showed highly directional migration, as seen qualitatively in the video data collected (Supplementary Videos 1 and 2) and in wind-rose plots of overlaid individual cell paths compared to DCs in collagen with no attractant present (Fig. 3C). As shown in Fig. 3D, although DCs migrated with similar velocities in the collagen matrix in the presence or absence of the attractant-releasing microspheres, the cells migrated with significantly greater directionality toward the attractant source gel in response to microsphere-generated gradients. Although the release rate of individual microspheres decays substantially over the timecourse of this assay, sustained DC attraction was observed throughout the 10 hr observation period. Strikingly, DCs near the attractant source gel at time zero migrated into the region where alginate microspheres were deposited and showed strong directional attraction right to the surface of individual CCL21-releasing particles (visualized by labeling DCs with a red cytosolic dye and loading the alginate particles with a fraction of Alexa Fluor 488-labeled CCL21, Fig. 3E). Thus, despite the presence of a field of overlapping gradients generated by the large collection of microspheres in the attractant gel, DCs still sensed and responded to local gradients around individual nearby microspheres. Altogether, these results suggest CCL21 released from the alginate particles was bioactive and strongly chemotactic for both human T-cells and dendritic cells.

3.3. Loading and sustained release of homeostatic and inflammatory chemokines from alginate microspheres

To be generally useful, this chemoattractant delivery approach should be capable of loading/releasing many different chemokines of interest for targeting different immune cell types. We thus tested the loading of several other host-derived attractant molecules in alginate microspheres, including CCL19, CXCL12, and CXCL10. CCL19, a second homeostatic ligand for CCR7, is expressed in lymph nodes [60, 61], and has a non-redundant role in lymphocyte homing [62]. CXCL12 is a lymphoid chemokine that attract T-cells, B-cells, and other immune cells [63], and CXCL10 is an IFN-γ-induced chemokine highly expressed at inflammatory sites, which attracts activated effector T-cells to sites of infection [64, 65]. As summarized in Table 1, these attractants have similar molecular weights, but differ in their net charge and net surface-exposed charge. For comparison with CCL21 loading/release from alginate particles, we measured the loading efficiency for two different attractant loading concentrations (Fig. 4A), and then measured release into serum-containing medium over time (Fig. 4B). The hierarchy of chemokine loading into the alginate particles was inverse to the release rate: CXCL12 loaded to the highest levels in the particles but also released extremely slowly from the particles. Although this remains a limited dataset, we found that for these four chemokines, the logarithm of the effective diffusivity of each chemokine in alginate (obtained by fitting the release data to a Fick's law model as in Fig. 2D) correlated well with the net surface charge of the proteins per residue (Fig. 4C), consistent with charge-mediated interactions between the attractants and alginate matrix dominating the loading/release behavior. These data suggest that alginate particles may be useful for engineering attractant gradients with a range of different candidate chemokines, though attractants with a very high surface charge density (e.g., CXCL12) may be bound too

tightly for effective gradient generation when loading into unmodified, highly charged alginate.

3.4. Chemotaxis responses to isolated chemokine-releasing microspheres

The experiments shown in Fig. 3B-E are a useful *in vitro* model of chemoattraction of cells to a site of particle deposition in tissue, as might be used in immunotherapy or vaccination. However, the striking local attraction of DCs to individual microspheres observed in these experiments prompted us to examine more closely the chemoattraction elicited by isolated individual microspheres, as a model for the response of leukocytes to isolated chemoattractant-releasing cells acting as a point source of chemokine. To this end, we first sought to measure and/or predict the concentration profiles of attractant generated around individual alginate microspheres loaded with CCL21. We first tried to directly visualize gradients around individual particles in collagen gels using fluorescently-labeled CCL21 as a tracer, but the minimum concentration of Alexa dye-labeled CCL21 that could be detected above background by either our widefield or confocal microscope systems was ~200 ng/ml, well above the concentration for chemotaxis observed in our collagen migration assays (data not shown). Thus, we instead used bulk measurements of chemokine release rates from collections of beads in suspension to model and predict the gradient expected around individual microspheres in collagen.

We simulated concentration fields evolving around individual microspheres using a 2D axis-symmetric model in which a microsphere was embedded in an 500 μm space (modeling alginate particles suspended in collagen at a concentration of 1×10^4 microspheres/ml); the chemokine was given an effective diffusivity in the alginate matrix D_{eff} as determined from our experimental bulk release data (e.g., Fig. 2D), while the diffusivity of chemokine in fibrillar collagen was taken as half its diffusivity in water [35, 36] (see Methods). From the chemokine concentration profiles, we also calculated the receptor occupancy gradient for cells located at any position along the chemokine gradient, as it the receptor occupancy gradient that determines signaling and directional migration [66].

The predicted concentration profiles and receptor occupancy gradients over time and space for a 50 μm diameter alginate particle initially loaded with 40 fg CCL21 (mimicking the loading achieved for incubations of 25 μg CCL21 per mg alginate) are plotted in Figs. 5A and 5B. The rapid diffusion of released CCL21 [35, 36] quickly dispersed chemokine throughout the simulation volume (Fig. 5A), while the decaying rate of chemokine release from microspheres over time led to chemokine concentration gradients (and thereby receptor occupancy gradients) that slowly decayed over the simulated timecourse (Fig. 5B). Prior studies [37, 67] have shown that leukocytes can sense and orient in response to a 2% change in chemokine concentration across the cell body (~10 μm) at optimal concentrations near K_d, and the threshold receptor occupancy difference for robust chemotactic migration has been estimated to be ~10 receptors across the length of a cell. This corresponds to a 0.033 – 0.1% change in receptor occupancy across the cell body for a lymphocyte expressing 10, 000 – 30, 000 chemokine receptors. Comparing the predicted receptor occupancy gradient to this threshold (expressed by the gray shaded area as a range covering physiological receptor expression levels, Fig. 5B), we see that over the first few hours the microsphere-generated gradient provides a detectable chemotactic stimulus for cells more than 150–200 μm away from the source. The model also predicts that by 5 hours, although the gradient has decayed at longer distances, a functional chemotactic gradient remains at distances 75–125 μm or less from the source. For comparison, we also modeled the concentration profile and receptor occupancy gradient evolution for CXCL12-releasing particles. For the same attractant loading conditions modeled above (25 μg CXCL12/mg alginate), the concentration gradient of CXCL12 (Fig. 5C) developing around an individual microsphere

was very shallow (less than 1% per 10 μm). Further, the receptor occupancy gradient was only beyond the estimated threshold within 50 μm of the microsphere surface (Fig. 5D).

To test whether this simple analysis of chemokine receptor engagement could accurately predict lymphocyte migration responses to chemokine-releasing microspheres, we imaged the response of activated T-cells to isolated CCL21- or CXCL12-releasing alginate microspheres in collagen gels, using experimental conditions matching as closely as possible the modeled conditions. Human T-cells were activated with PHA and IL-2; these cells expressed both CXCR4 and CCR7 (Supplementary Fig. 2B, C). As shown in Fig. 5E, activated T-cells suspended in collagen gels with CCL21-releasing alginate particles were attracted to individual microspheres from up to nearly 200 μm away. In the first hour, the mean chemotactic index (averaged values of the displacement of a given cell over a 1 min time interval toward the nearest particle divided by the total displacement) was on average greater than zero (indicating migration toward the nearest bead) for cells 150 μm or closer to attractant beads, and increased monotonically as the distance from the cell to nearest bead source decreased. After 4 hours, a similar trend of increasing chemotactic index with decreasing distance to the nearest bead held, but cells greater than 125 μm from the nearest bead exhibited a mean ICI which was not statistically different from zero. Thus, in line with the predictions from the simulation, the strength of the attractant gradient decayed and contracted around the microsphere over this 5-hr timecourse. By contrast, CXCL12-releasing alginate microspheres showed much weaker chemoattraction of T-cells, with some chemotaxis detected in the first hour, but no attraction by the second hour of observation (Fig. 5F). Thus, the simulations correctly captured the chemotaxis response of T-cells responding to CCL21-releasing particles, but did not predict the behavior of cells migrating near CXCL12-releasing microspheres. This outcome likely reflects the reductionist nature of the model employed here, which neglected receptor internalization and other modes of receptor desensitization that could be important for CXCL12-CXCR4 signaling.

4. Discussion

Chemokines control lymphocyte trafficking in health and disease, and are interesting candidates for therapeutic manipulation in vaccines and cancer immunotherapy. We previously showed that chemokines encapsulated in PLGA particles could create more sustainable and in some cases steeper chemoattractant concentration gradients within ECM gel models of tissue matrix compared to bolus soluble chemokine injections [20]. Here we sought to develop a more facile microsphere release system with greater control over the range of chemokines that could be functionally encapsulated and the dosages of attractant that could be loaded. We found the physical and chemical properties of alginate hydrogels particularly attractive in this setting: (i) The high hydrophilicity provides an environment that will preserve the bioactivity of encapsulated molecules; (ii) alginates form hydrogels under very mild gelation conditions permitting *in situ* loading of biomolecules if desired [68]; (iii) alginate has been used to carry cells and cytokines for therapeutic use due to its advantages of biocompatibility and mild processing conditions [68, 69]; and finally (iv) the anionic polysaccharide structure acts as a surrogate of extracellular GAGs to mimic reversible chemoattractant binding to the ECM.

Based on these considerations, we developed a post-synthesis adsorption approach to load chemoattractants into alginate microspheres, which provided several advantages over seeking to entrap chemokines during the particle preparation: Small single-use batches of attractant-loaded particles could be prepared, allowing efficient use of recombinant proteins; the attractants were not exposed to high shear or organic solvents used in the particle preparation; and a single homogeneous preparation of microspheres could be used for many independent experiments. Testing several different human chemokines, we found that these

basic proteins could be loaded to high levels in alginate particles, with release rates predicted by their net surface charge. Overall, loading/release measurements were consistent with a dominant role for electrostatics in mediating binding of the chemokines studied here to the alginate matrix, similar to binding of these largely cationic factors to GAGs in native ECM.

Cellular secretion rates for chemokines have been measured to range from 10^{-8} to 10^{-6} ng/hr/cell [70, 71]. However, these measurements are usually based on bulk measurements taken after prolonged culture periods of 24 or 48 hrs; while some chemokines are constitutively secreted, others are produced rapidly after stimulation within a brief time window (15 min – 1 hr) [72] and so these *in vitro* measurements may underestimate the production rate of chemokines. The maximum rates of cytokine secretion fall in the range of 2300–8000 molecules/cell·s [73] (estimated to be $1.65–5.74\times10^{-4}$ ng/cell·hr for CCL21). Here we found that alginate microspheres loaded with the human chemokines CCL21, CCL19, CXCL12 and CXCL10 released these attractants at rates ranging from 7.2×10^{-6} – 3.2×10^{-3} ng/hr/paritcle, covering the physiological range of chemokine release by individual cells. For CCL21, CCL19, and CXCL10, release rates in the physiological range were maintained for at least 24 hrs (data not shown).

We used modified Boyden chamber assays and direct videomicroscopy analysis of cells migrating in collagen to assess the bioactivity of alginate-released chemokines, and found in both assays evidence of potent chemoattraction elicited by particle-released chemokine. The striking attraction of dendritic cells to individual alginate microspheres in the conjoined gel assay prompted us to explore in more detail cell migration near individual cell-sized attractant sources. The ability to experimentally define (and manipulate) the attractant release rate from these microspheres provides the opportunity to dissect how immune cells interpret local attractant gradients in a manner that would be challenging to achieve using live cells as chemokine sources. We analyzed the migration response of activated T-cells toward microspheres releasing CCL21 or CXCL12, as these two attractants were distinguished by moderate and very slow release kinetics, respectively. Because direct visualization of chemokine gradients proved to be problematic, we used measurements of chemokine release coupled with careful characterization of the microsphere size distribution (because particle size influences the rate of chemokine freed at the particle surfaces) to provide experimental data guiding simulations of attractant gradient evolution around isolated microparticles. The modeling semi-quantitatively predicted the responsiveness of T-cells to CCL21-releasing microspheres, with the chemoattracting “reach” of the microspheres initially drawing in cells from nearly 200 μm away, but collapsing toward the source particle slowly over the course of hours. By contrast, T-cell migration toward CXCL12-releasing microspheres was transient, with chemotaxis of cells up to 125 μm away at the start of the experiment but no attraction detected after 1 hr. The simple diffusion-based modeling of the CXCL12 gradient predicted that some attraction should have been sustained near the beads. The good agreement of responses seen for CCL21 and relative lack of agreement for the model with CXCL12 migration data likely reflects the key difference in receptor biology for these two ligands; CCL21 bound to CCR7 does not trigger receptor downregulation or desensitization [74, 75], while CXCL12 triggers rapid receptor internalization [76, 77]. The loss of receptors from the cell surface raises the effective threshold in receptor occupancy that must be met for directional migration, likely ablating chemotaxis for cells in CXCL12 gradients over time.

For some applications, it would be desirable to modulate the release rate of individual chemokines independent of the quantity of attractant loaded. Several strategies could provide this level of control: (i) varying the density of alginate or calcium content in the hydrogel microspheres [78]; (ii) adding additives that alter protein binding [30]; or (iii)

derivatizing carboxyl functional groups on the alginate chains to alternate functional groups that could exhibit enhanced or reduced binding [79]. The flexibility of tuning release properties of chemokines from alginate microspheres would make it a further attractive method of delivery chemokines for therapeutic use and chemotaxis studies.

5. Conclusions

The development of versatile chemoattractant carrier systems is of interest for both therapeutic applications and fundamental chemotaxis studies. Here we have shown that alginate hydrogel microspheres can be efficiently loaded with a range of different chemokines and release bioactive protein generating functional attractant gradients both in 2D medium and 3D collagen ECM gels. We have also demonstrated the use of chemokine loaded alginate microspheres as model attractant “point sources” to investigate the chemotaxis behavior of activated human T-cells and showed that a simple diffusion-based modeling of the concentration profile and resulting receptor occupancy gradient could predict chemotactic behavior for an attractant receptor which does not undergo internalization/desensitization. We thus believe that this alginate hydrogel microsphere system could be useful in *in vitro* and *in vivo* chemotaxis studies, and possibly in immunotherapy and vaccine delivery by attracting target effector cells to desired tissue sites. More generally, attractants involved in developmental, wound healing, and tissue regeneration processes could be delivered using this approach to engineer chemotaxis of many cell types *in vitro* and *in vivo*.

Supplementary Material

Refer to Web version on PubMed Central for supplementary material.

Acknowledgments

This work was supported in part by Defense Advanced Research Projects Agency (DARPA) and NIH (1R01EB007280). D.J.I. is an investigator of the Howard Hughes Medical Institute.

References

1. Campbell DJ, Kim CH, Butcher EC. Chemokines in the systemic organization of immunity. Immunol Rev. 2003; 195:58–71. [PubMed: 12969310]
2. Kim CH, Broxmeyer HE. Chemokines: signal lamps for trafficking of T and B cells for development and effector function. J Leukoc Biol. 1999; 65:6–15. [PubMed: 9886241]
3. Olson TS, Ley K. Chemokines and chemokine receptors in leukocyte trafficking. Am J Physiol Regul Integr Comp Physiol. 2002; 283:R7–28. [PubMed: 12069927]
4. Wei SH, Parker I, Miller MJ, Cahalan MD. A stochastic view of lymphocyte motility and trafficking within the lymph node. Immunol Rev. 2003; 195:136–59. [PubMed: 12969316]
5. Miyasaka M, Tanaka T. Lymphocyte trafficking across high endothelial venules: dogmas and enigmas. Nat Rev Immunol. 2004; 4:360–70. [PubMed: 15122201]
6. Rot A, von Andrian UH. Chemokines in innate and adaptive host defense: basic chemokinese grammar for immune cells. Annu Rev Immunol. 2004; 22:891–928. [PubMed: 15032599]
7. Devreotes PN, Zigmond SH. Chemotaxis in eukaryotic cells: a focus on leukocytes and Dictyostelium. Annu Rev Cell Biol. 1988; 4:649–86. [PubMed: 2848555]
8. Lauffenburger DA, Horwitz AF. Cell migration: a physically integrated molecular process. Cell. 1996; 84:359–69. [PubMed: 8608589]
9. Stachowiak AN, Wang Y, Huang YC, Irvine DJ. Homeostatic lymphoid chemokines synergize with adhesion ligands to trigger T and B lymphocyte chemokinesis. J Immunol. 2006; 177:2340–8. [PubMed: 16887995]

10. Houshmand P, Zlotnik A. Therapeutic applications in the chemokine superfamily. Curr Opin Chem Biol. 2003; 7:457–60. [PubMed: 12941419]
11. Toka FN, Gierynska M, Rouse BT. Codelivery of CCR7 ligands as molecular adjuvants enhances the protective immune response against herpes simplex virus type 1. J Virol. 2003; 77:12742–52. [PubMed: 14610196]
12. Kirk CJ, Hartigan-O'Connor D, Mule JJ. The dynamics of the T-cell antitumor response: chemokine-secreting dendritic cells can prime tumor-reactive T cells extranodally. Cancer Res. 2001; 61:8794–802. [PubMed: 11751401]
13. Guiducci C, Di Carlo E, Parenza M, Hitt M, Giovarelli M, Musiani P, et al. Intralesional injection of adenovirus encoding CC chemokine ligand 16 inhibits mammary tumor growth and prevents metastatic-induced death after surgical removal of the treated primary tumor. J Immunol. 2004; 172:4026–36. [PubMed: 15034014]
14. Yang SC, Hillinger S, Riedl K, Zhang L, Zhu L, Huang M, et al. Intratumoral administration of dendritic cells overexpressing CCL21 generates systemic antitumor responses and confers tumor immunity. Clin Cancer Res. 2004; 10:2891–901. [PubMed: 15102698]
15. Thanarajasingam U, Sanz L, Diaz R, Qiao J, Sanchez-Perez L, Kottke T, et al. Delivery of CCL21 to metastatic disease improves the efficacy of adoptive T-cell therapy. Cancer Res. 2007; 67:300–8. [PubMed: 17210711]
16. Guiducci C, Vicari AP, Sangaletti S, Trinchieri G, Colombo MP. Redirecting in vivo elicited tumor infiltrating macrophages and dendritic cells towards tumor rejection. Cancer Res. 2005; 65:3437–46. [PubMed: 15833879]
17. Kumamoto T, Huang EK, Paek HJ, Morita A, Matsue H, Valentini RF, et al. Induction of tumor-specific protective immunity by in situ Langerhans cell vaccine. Nat Biotechnol. 2002; 20:64–9. [PubMed: 11753364]
18. Singh A, Suri S, Roy K. In-situ crosslinking hydrogels for combinatorial delivery of chemokines and siRNA-DNA carrying microparticles to dendritic cells. Biomaterials. 2009; 30:5187–200. [PubMed: 19560815]
19. Kress H, Park JG, Mejean CO, Forster JD, Park J, Walse SS, et al. Cell stimulation with optically manipulated microsources. Nat Methods. 2009; 6:905–9. [PubMed: 19915561]
20. Zhao X, Jain S, Benjamin Larman H, Gonzalez S, Irvine DJ. Directed cell migration via chemoattractants released from degradable microspheres. Biomaterials. 2005; 26:5048–63. [PubMed: 15769541]
21. Tamber H, Johansen P, Merkle HP, Gander B. Formulation aspects of biodegradable polymeric microspheres for antigen delivery. Adv Drug Deliv Rev. 2005; 57:357–76. [PubMed: 15560946]
22. van de Weert M, Hennink WE, Jiskoot W. Protein instability in poly(lactic-co-glycolic acid) microparticles. Pharm Res. 2000; 17:1159–67. [PubMed: 11145219]
23. Zhu G, Mallery SR, Schwendeman SP. Stabilization of proteins encapsulated in injectable poly (lactide- co-glycolide). Nat Biotechnol. 2000; 18:52–7. [PubMed: 10625391]
24. Hori Y, Winans AM, Irvine DJ. Modular injectable matrices based on alginate solution/ microsphere mixtures that gel in situ and co-deliver immunomodulatory factors. Acta Biomater. 2009; 5:969–82. [PubMed: 19117820]
25. Hori Y, Winans AM, Huang CC, Horrigan EM, Irvine DJ. Injectable dendritic cell-carrying alginate gels for immunization and immunotherapy. Biomaterials. 2008; 29:3671–82. [PubMed: 18565578]
26. Proudfoot AE, Handel TM, Johnson Z, Lau EK, LiWang P, Clark-Lewis I, et al. Glycosaminoglycan binding and oligomerization are essential for the in vivo activity of certain chemokines. Proc Natl Acad Sci U S A. 2003; 100:1885–90. [PubMed: 12571364]
27. Wagner L, Yang OO, Garcia-Zepeda EA, Ge Y, Kalams SA, Walker BD, et al. Beta-chemokines are released from HIV-1-specific cytolytic T-cell granules complexed to proteoglycans. Nature. 1998; 391:908–11. [PubMed: 9495345]
28. Ali S, Robertson H, Wain JH, Isaacs JD, Malik G, Kirby JA. A non-glycosaminoglycan-binding variant of CC chemokine ligand 7 (monocyte chemoattractant protein-3) antagonizes chemokine-mediated inflammation. J Immunol. 2005; 175:1257–66. [PubMed: 16002730]

29. Edelman ER, Mathiowitz E, Langer R, Klagsbrun M. Controlled and modulated release of basic fibroblast growth factor. Biomaterials. 1991; 12:619–26. [PubMed: 1742404]
30. Mumper RJ, Hoffman AS, Puolakkainen PA, Bouchard LS, Gombotz WR. Calcium-alginate beads for the oral delivery of transforming growth factor-β1 (TGF-β1): stabilization of TGF-β1 by the addition of polyacrylic acid within acid-treated beads. J Control Release. 1994; 30:241–51.
31. Maysinger D, Jalsenjak I, Cuello AC. Microencapsulated nerve growth factor: effects on the forebrain neurons following devascularizing cortical lesions. Neurosci Lett. 1992; 140:71–4. [PubMed: 1407703]
32. Liao IC, Wan AC, Yim EK, Leong KW. Controlled release from fibers of polyelectrolyte complexes. J Control Release. 2005; 104:347–58. [PubMed: 15907585]
33. Yang D, Chen Q, Hoover DM, Staley P, Tucker KD, Lubkowski J, et al. Many chemokines including CCL20/MIP-3alpha display antimicrobial activity. J Leukoc Biol. 2003; 74:448–55. [PubMed: 12949249]
34. Crank, J. The Mathematics of Diffusion. Oxford: Clarendon Press; 1975.
35. Lauffenburger DA, Tranquillo RT, Zigmond SH. Concentration gradients of chemotactic factors in chemotaxis assays. Methods Enzymol. 1988; 162:85–101. [PubMed: 3226329]
36. Tanford, C. Physcial Chemistry of Macromolecules. New York: Wiley; 1961.
37. Zigmond SH. Ability of polymorphonuclear leukocytes to orient in gradients of chemotactic factors. J Cell Biol. 1977; 75:606–16. [PubMed: 264125]
38. Campbell JJ, Bowman EP, Murphy K, Youngman KR, Siani MA, Thompson DA, et al. 6-C-kine (SLC), a lymphocyte adhesion-triggering chemokine expressed by high endothelium, is an agonist for the MIP-3beta receptor CCR7. J Cell Biol. 1998; 141:1053–9. [PubMed: 9585422]
39. Willimann K, Legler DF, Loetscher M, Roos RS, Delgado MB, Clark-Lewis I, et al. The chemokine SLC is expressed in T cell areas of lymph nodes and mucosal lymphoid tissues and attracts activated T cells via CCR7. Eur J Immunol. 1998; 28:2025–34. [PubMed: 9645384]
40. Yoshida R, Nagira M, Imai T, Baba M, Takagi S, Tabira Y, et al. EBI1-ligand chemokine (ELC) attracts a broad spectrum of lymphocytes: activated T cells strongly up-regulate CCR7 and efficiently migrate toward ELC. Int Immunol. 1998; 10:901–10. [PubMed: 9701028]
41. Burns JM, Summers BC, Wang Y, Melikian A, Berahovich R, Miao Z, et al. A novel chemokine receptor for SDF-1 and I-TAC involved in cell survival, cell adhesion, and tumor development. J Exp Med. 2006; 203:2201–13. [PubMed: 16940167]
42. Balabanian K, Lagane B, Infantino S, Chow KY, Harriague J, Moepps B, et al. The chemokine SDF-1/CXCL12 binds to and signals through the orphan receptor RDC1 in T lymphocytes. J Biol Chem. 2005; 280:35760–6. [PubMed: 16107333]
43. Moghe PV, Nelson RD, Tranquillo RT. Cytokine-stimulated chemotaxis of human neutrophils in a 3-D conjoined fibrin gel assay. J Immunol Methods. 1995; 180:193–211. [PubMed: 7714334]
44. Hori Y, Stern PJ, Hynes RO, Irvine DJ. Engulfing tumors with synthetic extracellular matrices for cancer immunotherapy. Biomaterials. 2009; 30:6757–67. [PubMed: 19766305]
45. Tanaka Y, Adams DH, Hubscher S, Hirano H, Siebenlist U, Shaw S. T-cell adhesion induced by proteoglycan-immobilized cytokine MIP-1 beta. Nature. 1993; 361:79–82. [PubMed: 7678446]
46. Hoogewerf AJ, Kuschert GS, Proudfoot AE, Borlat F, Clark-Lewis I, Power CA, et al. Glycosaminoglycans mediate cell surface oligomerization of chemokines. Biochemistry. 1997; 36:13570–8. [PubMed: 9354625]
47. Patel DD, Koopmann W, Imai T, Whichard LP, Yoshie O, Krangel MS. Chemokines have diverse abilities to form solid phase gradients. Clin Immunol. 2001; 99:43–52. [PubMed: 11286540]
48. Nakano H, Tamura T, Yoshimoto T, Yagita H, Miyasaka M, Butcher EC, et al. Genetic defect in T lymphocyte-specific homing into peripheral lymph nodes. Eur J Immunol. 1997; 27:215–21. [PubMed: 9022021]
49. Stein JV, Rot A, Luo Y, Narasimhaswamy M, Nakano H, Gunn MD, et al. The CC chemokine thymus-derived chemotactic agent 4 (TCA-4, secondary lymphoid tissue chemokine, 6Ckine, exodus-2) triggers lymphocyte function-associated antigen 1-mediated arrest of rolling T lymphocytes in peripheral lymph node high endothelial venules. J Exp Med. 2000; 191:61–76. [PubMed: 10620605]

50. Worbs T, Mempel TR, Bolter J, von Andrian UH, Forster R. CCR7 ligands stimulate the intranodal motility of T lymphocytes in vivo. J Exp Med. 2007; 204:489–95. [PubMed: 17325198]
51. Forster R, Schubel A, Breitfeld D, Kremmer E, Renner-Muller I, Wolf E, et al. CCR7 coordinates the primary immune response by establishing functional microenvironments in secondary lymphoid organs. Cell. 1999; 99:23–33. [PubMed: 10520991]
52. Gunn MD, Kyuwa S, Tam C, Kakiuchi T, Matsuzawa A, Williams LT, et al. Mice lacking expression of secondary lymphoid organ chemokine have defects in lymphocyte homing and dendritic cell localization. J Exp Med. 1999; 189:451–60. [PubMed: 9927507]
53. Hirose J, Kawashima H, Willis MS, Springer TA, Hasegawa H, Yoshie O, et al. Chondroitin sulfate B exerts its inhibitory effect on secondary lymphoid tissue chemokine (SLC) by binding to the C-terminus of SLC. Biochimica et Biophysica Acta. 2002; 1571:219–24. [PubMed: 12090936]
54. Christopherson KW 2nd, Campbell JJ, Travers JB, Hromas RA. Low-molecular-weight heparins inhibit CCL21-induced T cell adhesion and migration. J Pharmacol Exp Ther. 2002; 302:290–5. [PubMed: 12065729]
55. Castro GR, Chen J, Panilaitis B, Kaplan DL. Emulsan-alginate beads for protein adsorption. J Biomater Sci Polym Ed. 2009; 20:411–26. [PubMed: 19228444]
56. Admason, AW. Physical Chemistry of Surfaces. New York: John Wiley and Sons; 1976.
57. Kwon GS, Bae YH, Cremers H, Feijen J, Kim SW. Release of proteins via ion exchange from albumin-heparin microspheres. J Control Release. 1992; 22:83–94.
58. Tayalia P, Mazur E, Mooney DJ. Controlled architectural and chemotactic studies of 3D cell migration. Biomaterials. 2011; 32:2634–41. [PubMed: 21237507]
59. Schumann K, Lammermann T, Bruckner M, Legler DF, Polleux J, Spatz JP, et al. Immobilized chemokine fields and soluble chemokine gradients cooperatively shape migration patterns of dendritic cells. Immunity. 2010; 32:703–13. [PubMed: 20471289]
60. Kim CH, Pelus LM, White JR, Applebaum E, Johanson K, Broxmeyer HE. CK beta-11/macrophage inflammatory protein-3 beta/EBI1-ligand chemokine is an efficacious chemoattractant for T and B cells. J Immunol. 1998; 160:2418–24. [PubMed: 9498785]
61. Ngo VN, Tang HL, Cyster JG. Epstein-Barr virus-induced molecule 1 ligand chemokine is expressed by dendritic cells in lymphoid tissues and strongly attracts naive T cells and activated B cells. J Exp Med. 1998; 188:181–91. [PubMed: 9653094]
62. Link A, Vogt TK, Favre S, Britschgi MR, Acha-Orbea H, Hinz B, et al. Fibroblastic reticular cells in lymph nodes regulate the homeostasis of naive T cells. Nat Immunol. 2007; 8:1255–65. [PubMed: 17893676]
63. Bleul CC, Fuhlbrigge RC, Casasnovas JM, Aiuti A, Springer TA. A highly efficacious lymphocyte chemoattractant, stromal cell-derived factor 1 (SDF-1). J Exp Med. 1996; 184:1101–9. [PubMed: 9064327]
64. Farber JM. Mig and IP-10: CXC chemokines that target lymphocytes. J Leukoc Biol. 1997; 61:246–57. [PubMed: 9060447]
65. Taub DD, Lloyd AR, Wang JM, Oppenheim JJ, Kelvin DJ. The effects of human recombinant MIP-1 alpha, MIP-1 beta, and RANTES on the chemotaxis and adhesion of T cell subsets. Adv Exp Med Biol. 1993; 351:139–46. [PubMed: 7524282]
66. Herzmark P, Campbell K, Wang F, Wong K, El-Samad H, Groisman A, et al. Bound attractant at the leading vs. the trailing edge determines chemotactic prowess. P Natl Acad Sci USA. 2007; 104:13349–54.
67. Lin F, Butcher EC. Modeling the role of homologous receptor desensitization in cell gradient sensing. J Immunol. 2008; 181:8335–43. [PubMed: 19050250]
68. Wee S, Gombotz WR. Protein release from alginate matrices. Adv Drug Deliv Rev. 1998; 31:267–85. [PubMed: 10837629]
69. Kong, HJ.; Mooney, DJ. Polysaccharides. 2. Marcel & Dekker; 2005. Polysaccharide hydrogels in tissue engineering.
70. Chieppa M, Bianchi G, Doni A, Del Prete A, Sironi M, Laskarin G, et al. Cross-linking of the mannose receptor on monocyte-derived dendritic cells activates an anti-inflammatory immunosuppressive program. J Immunol. 2003; 171:4552–60. [PubMed: 14568928]

71. Lebre MC, Burwell T, Vieira PL, Lora J, Coyle AJ, Kapsenberg ML, et al. Differential expression of inflammatory chemokines by Th1- and Th2-cell promoting dendritic cells: a role for different mature dendritic cell populations in attracting appropriate effector cells to peripheral sites of inflammation. Immunol Cell Biol. 2005; 83:525–35. [PubMed: 16174103]

72. Oynebraten I, Bakke O, Brandtzaeg P, Johansen FE, Haraldsen G. Rapid chemokine secretion from endothelial cells originates from 2 distinct compartments. Blood. 2004; 104:314–20. [PubMed: 15044249]

73. Francis K, Palsson BO. Effective intercellular communication distances are determined by the relative time constants for cyto/chemokine secretion and diffusion. Proc Natl Acad Sci U S A. 1997; 94:12258–62. [PubMed: 9356436]

74. Kohout TA, Nicholas SL, Perry SJ, Reinhart G, Junger S, Struthers RS. Differential desensitization, receptor phosphorylation, beta-arrestin recruitment, and ERK1/2 activation by the two endogenous ligands for the CC chemokine receptor 7. J Biol Chem. 2004; 279:23214–22. [PubMed: 15054093]

75. Otero C, Groettrup M, Legler DF. Opposite fate of endocytosed CCR7 and its ligands: recycling versus degradation. J Immunol. 2006; 177:2314–23. [PubMed: 16887992]

76. Haribabu B, Richardson RM, Fisher I, Sozzani S, Peiper SC, Horuk R, et al. Regulation of human chemokine receptors CXCR4. Role of phosphorylation in desensitization and internalization. J Biol Chem. 1997; 272:28726–31. [PubMed: 9353342]

77. Signoret N, Oldridge J, Pelchen-Matthews A, Klasse PJ, Tran T, Brass LF, et al. Phorbol esters and SDF-1 induce rapid endocytosis and down modulation of the chemokine receptor CXCR4. J Cell Biol. 1997; 139:651–64. [PubMed: 9348282]

78. Silva CM, Ribeiro AJ, Figueiredo IV, Goncalves AR, Veiga F. Alginate microspheres prepared by internal gelation: development and effect on insulin stability. Int J Pharm. 2006; 311:1–10. [PubMed: 16442757]

79. Polyak B, Geresh S, Marks RS. Synthesis and characterization of a biotin-alginate conjugate and its application in a biosensor construction. Biomacromolecules. 2004; 5:389–96. [PubMed: 15002998]

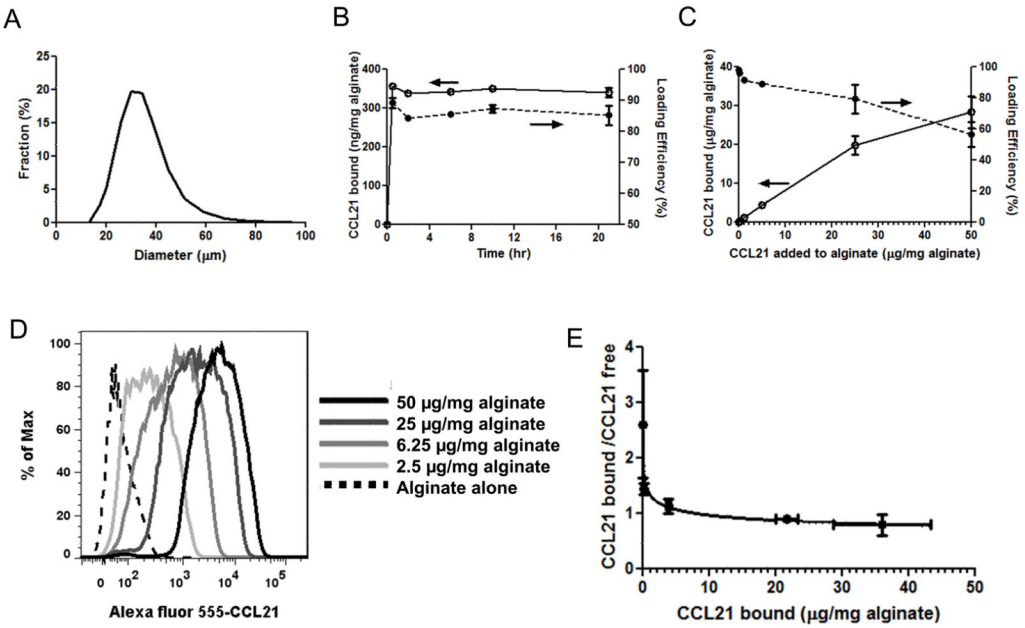

Fig. 1. Characterization of alginate hydrogel microspheres and chemokine loading

(A) Size distribution of alginate particles determined by laser diffraction. (B) The net amount of chemokine bound and percentage of added chemokine adsorbed by alginate microspheres (loading efficiency) were quantified as a function of incubation time for 5×10^6 particles/ml incubated with 20 μg/ml CCL21 (equivalent to 0.4 μg CCL21/mg alginate) up to 24 hrs. (C) Loading efficiency and net quantity of CCL21 loaded into alginate microspheres incubated for 90 min with varying doses of chemokine. (D) Flow cytometry analysis of microspheres showing binding of Alexa fluor 555-labeled CCL21 to particles following incubation of microspheres with indicated Alexa 555-CCL21 doses for 90 min. (E) Scatchard plot of CCL21 adsorption to alginate microspheres. Data were fit to the Freundlich model for adsorption (solid line). Data shown are means ± SE.

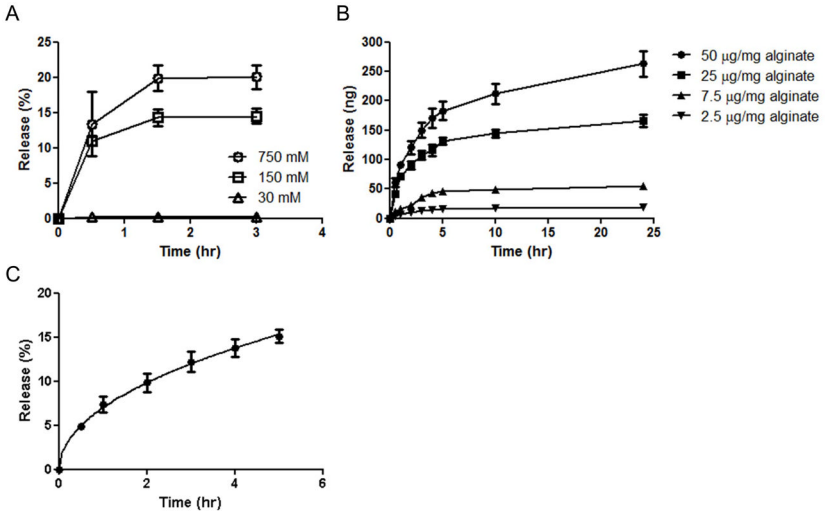

Fig. 2. Kinetics of CCL21 release from alginate microspheres

(A) Impact of medium ionic strength on rate of CCL21 release from alginate particles (particles loaded at 25 μg CCL21/mg alginate for 90 min) incubated in 10 mM PBS pH 7.4, 2 mM $CaCl_2$, 1% BSA medium containing the indicated concentrations of NaCl at 37°C. (B) Kinetics of CCL21 release from alginate particles into RPMI medium with 10% FCS at 37°C as a function of quantity of chemokine added to alginate during loading. (C) Fractional release of CCL21 vs. time fit to a simple diffusion model (solid line), for particles incubated with 25 μg CCL21/mg alginate during loading. Data shown are means ± SE.

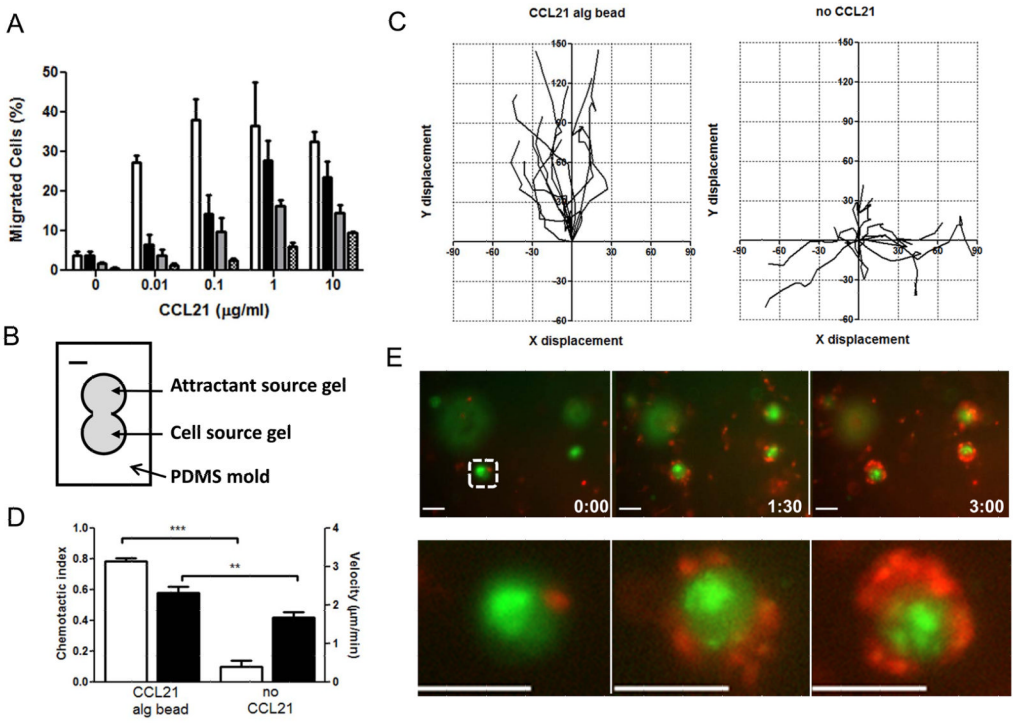

Fig. 3. Bioactivity of CCL21 released from alginate microspheres

(A) Percentage of resting human T-cells migrating through filters in response to different total doses of CCL21 provided in soluble or microsphere form in a modified Boyden chamber chemotaxis assay; incubations were carried out for 2 hr (cells applied to filter plates in medium) or 4 hr (cells applied to filter plates in collagen gels). Open bars, soluble CCL21 with cells in medium; black bars, soluble CCL21 with cells in collagen; gray bars, microspheres with CCL21 and cells in medium; hatched bars, microspheres with CCL21 and cells in collagen. (B)–(E) Conjoined collagen gel chemotaxis assay with LPS-activated human dendritic cells in a "cell source" gel migrating toward an "attractant source" gel loaded at time zero with 0.8 μg CCL21 in 5×10^4 alginate microspheres or control gels lacking attractant. (B) Schematic of conjoined gel assay setup; scale bar is 2 mm. (C) Wind-rose 2D plots of individual DC migration paths tracked 3–6 hr after start of the assay, for cells located 1 mm from the center of the conjoined gel; each track length is 60 min; x-y axes are cell displacements from their starting position at the beginning of the time interval in μm. (D) Average chemotactic index (open bars) and velocity of DCs (filled bars) (n = 20 cells analyzed for each condition; unpaired t test: *** $P<0.0001$). (E) Migrating DCs (red) entering the "attractant source" gel migrated directly into contact with individual CCL21 alginate microspheres (marked by Alexa-fluor-tagged CCL21, green); Lower panels show zoomed-in view of individual microsphere highlighted by the dashed box in upper panel series; scale bar is 50 μm.

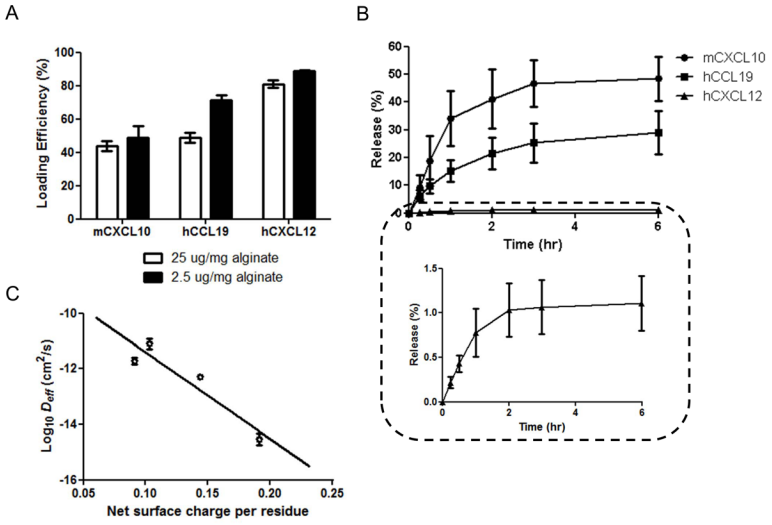

Fig. 4. Loading and release of CXCL12, CCL19 and CXCL10 from alginate microspheres

(A) Loading efficiency of chemokines in microspheres was measured following incubation of 2.5 or 25 μg chemokine/mg alginate for 90 min. (B) Kinetics of chemokine release into serum-containing medium at 37°C for particles incubated with 25 μg chemokine/mg alginate during loading. (C) Logarithm of effective diffusivity of chemokines in alginate as a function of net surface charge per residue, with best fit linear regression. Data shown are mean ± SE.

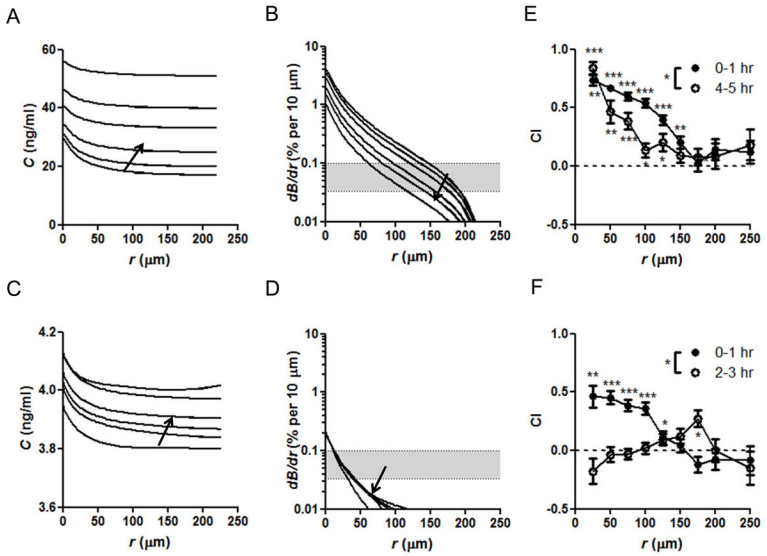

Fig. 5. Relationship between microsphere-generated chemoattractant gradients, receptor occupancy, and migration responses

(A–D) Simulated chemokine concentration gradients developed around an isolated 50 μm-diameter alginate microsphere releasing CCL21 (A, B) or CXCL12 (C, D), calculated from experimentally-determined release rates of particles incubated with 25 μg chemokine/mg alginate during loading. Shown are the chemoattractant concentration (*C*) (A, C) and chemokine receptor occupancy gradients (*dB/dr*) as a function of distance to the surface of microsphere (*r*) (B, D) at 15 min, 0.5 hr, 1 hr, 2 hr, 3 hr, and 5 hr; arrows indicate the trend of increasing time. Shaded areas in B, D indicate the estimated threshold of gradients in receptor occupancy required for directional migration for cells expressing 10, 000 to 30, 000 receptors. (E, F) Mean chemotactic index (CI) of activated human T-cells migrating through collagen gels in the vicinity of isolated microspheres releasing CCL21 (E) or CXCL12 (F) as a function of distance from the microspheres (*r*); shown are mean CI ± SE determined from 1-min time steps of cells analyzed in the indicated window of time after start of the experiment; dashed lines indicate the expected CI for random migration (zero); values significantly different from zero are indicated: * P<0.5, ** P<0.001, *** P<0.0001. CIs determined for (E) *n* = 107 cells (0–1 hr) and *n* = 45 cells (4–5 hr); * P<0.05; (F) *n* = 67 cells (0–1 hr) and *n* = 59 cells (2–3 hr); * P<0.05.

Table 1

Chemokine physicochemical properties

	CXCL12	CCL21	CCL19	CXCL10
Molecular weight (kDa)	7.96	12.25	8.80	8.70
Net charge	+9	+16	+7	+9
Isoelectric point	10.3	10.5	10.1	10.5
Surface positive charge	+13	+25	+13	+13
Surface negative charge	0	−9	−6	−5
Net surface charge per residue	0.19	0.14	0.09	0.10